Vertical free-standing films of amphiphilic associating polyelectrolytes

F. Millet and J. J. Benattar
Service de Physique de l'Etat Condensé, Centre d'Etude de Saclay, F-91191 Gif sur Yvette Cedex, France

P. Perrin
ESPCI, CNRS, UPMC, UMR 7615, Physico-chimie des Polymères 10, rue Vauquelin, 75005 Paris, France
(Received 28 December 1998)

Hydrophobically modified poly(acrylic acid) sodium salt (HMPAANa) copolymers are known to provide a huge stabilization of oil in water macroemulsions. An interstitial HMPAANa film is formed between the oil droplets, thus creating repulsion between them. We present an x-ray reflectivity study of vertical free-standing films drawn from aqueous solutions of HMPAANa copolymers. The vertical HMPAANa films are model systems for the interstitial films between oil droplets and the description of their behavior provides information about the stabilization process. Their thickness was investigated as a function of various parameters such as the solution concentration, the degree of grafting, the length of the grafts, and the backbone molecular weight. Below a solution concentration threshold (C_t), the film thickness scales like the square root of the molecular weight and is independent of the degree of grafting and the length of the grafts. Polyelectrolyte chains adopt a self-screened coil conformation within the films and the thickness is governed by the radius of gyration of the coils. Above C_t, a transition from a bimolecular film to a physical gel is observed and the thickness then increases with concentration. Finally, we propose an explanation for the stabilization of macroemulsions by HMPAANa copolymers. [S1063-651X(99)10308-8]

PACS number(s): 68.15.+e, 36.20.Ey, 61.25.Hq

I. INTRODUCTION

Amphiphilic associating polyelectrolytes are known to be very efficient stabilizers of oil in water macroemulsions [1,2]. Indeed, very large oil droplets with diameter of about 10 μm are stable for months in water when stabilized by hydrophobically modified poly(acrylic acid) sodium salt (HMPAANa) copolymers. Hydrophobic monomers anchor in the nonpolar droplets, thus diminishing the surface tension, while the soluble polyelectrolyte backbones surround the droplets in the aqueous medium. As the droplets are submitted to gravitational forces, they collect in a creamed layer at the top of the solution and come very close to each under the effect of flocculation. At this point, an interstitial aqueous HMPAANa polymer film is formed between close-packed droplets and the adsorbed copolymer molecules give rise to repulsion forces between droplets. This repulsion, which is thought to be both steric and electrostatic [3], prevents the droplets from coalescing and then enhances considerably the stability of the macroemulsions. The description of the behavior of polyelectrolyte films is then of crucial importance for the understanding of the stabilization process.

Indeed, the question of polymers at interfaces or within films has been broadly studied. The concentration profile and thickness of an adsorbed polymer layer at the air/water interface and the interaction between two plates carrying polymers have been calculated [4–7] and measured [8–13]. The adsorbed polymer molecules form a fluffy layer at the interface consisting of trains (monomers in direct contact with the surface), loops and tails (polymer chain ends) [4–6]. The thickness of the adsorbed layer is controlled by the longest loops and tails and scales like the radius of gyration of the polymer. In the case of neutral polymers attached by only one end at an interface, the existence of a stretched regime has been predicted [7] and experimentally evidenced [13]. Above a certain density of attachment points, the polymer chains are stretched and the thickness of the adsorbed layer scales like the linear length of the polymer. Force-measurement experiments on aqueous amphiphilic polymer films revealed that the repulsive forces between the surfaces of a polymer film showed an exponential decay with a characteristic length proportional to the radius of gyration of the free polymer chain in solution [12]. This was in good agreement with theoretical results [6].

We present in this paper a complete investigation of the behavior of vertical free-standing films drawn from HMPAANa solutions with the x-ray reflectivity technique. These films provide an appropriate model system to describe the interstitial films separating oil droplets and x-ray reflectivity is a very appropriate technique for the study of soap films. Indeed, this technique has already given an accurate description of the Newton black film made of small-molecule surfactants [14]. It is composed of two amphiphilic layers only separated by a hydration layer of the surfactant polar heads. X-ray reflectivity has also given a good description of the behavior of vertical free-standing films composed of two charged brushes in interaction as a function of the electrolyte concentration [15]. In the present study, we have investigated the influence of every available parameter on the HMPAANa films: the concentration of the solution, the degree of grafting of the polyelectrolyte, the length of the grafts, and the molecular weight of the polyelectrolyte backbone. We show that the film thickness is controlled by the radius of gyration and the associative properties of the polymer. Finally, we propose a qualitative explanation for the huge stabilization of macroemulsions by HMPAANa.

II. MATERIALS

The synthesis of HMPAANa has been already described elsewhere [16]. Hydrophobic alkyl chains (*n*-dodecyl or *n*-octadecyl) are randomly grafted onto the negatively charged water-soluble backbone:

$$[(CH_2CH)CO_2Na]_{100-\tau}[(CH_2CH)CONH(CH_2)_{n-1}CH_3]_{100-\tau}.$$

The chemical structure of the grafted polyelectrolytes can be adjusted by changing the degree of grafting ($\tau = 1$, 3, and 10 mol%), the number of carbon atoms in the alkyl chains ($n = 12$ and 18) and the weight average molecular weight ($M_w = 18\,000$, $34\,000$, $120\,000$, and $525\,000$ g/mol) measured within an error of 10% by size exclusion chromatography (SEC) measurements. The polydispersity index ranges from 1.2 for the lowest molecular weight to 4 for the highest one. For the sake of clarity, the modified polymers are referred to as ($M_W \times 10^{-3}$) τCn, where C_n means that the alkyl grafts are composed of n carbon atoms. The degree of grafting was determined by ^{1}H NMR spectroscopy and elemental analysis. Aqueous solutions were prepared with double distilled deionized water with a milli-Q system (Millipore).

The behavior of associating polymers in water is now briefly described. At polymer concentrations higher than the critical aggregate concentration (cac), alkyl grafts aggregate to protect themselves from water. This hydrophobic aggregation process, which has been extensively characterized [17], leads to intermolecular associations and to the formation of a physical network. The viscosity of the solutions then rapidly increases above the cac. The cac of the HMPAANa copolymers were determined by both viscometry [1,2,16] and surface tension measurements [18].

III. METHOD AND EQUIPMENT

A x-ray reflectivity experiment consists of the measurement of the ratio $R(\theta) = I(\theta)/I_0$, where $I(\theta)$ is the intensity of the specular beam reflected by a surface at an angle θ and I_0 that of the incident beam. The wave-vector transfer $\mathbf{q}$ is perpendicular to the surface and the analysis of the reflectivity curves provides information about the mean electron density along the normal z to the surface. The refractive index is given by $n = 1 - \delta - i\beta$, where δ is proportional to the electron density:

$$\delta(z) = \frac{\lambda^2}{2\pi} r_e \rho(z), \tag{1}$$

where λ is the x-ray wavelength, r_e is the classical radius of the electron, $\rho(z)$ is the electron density along the z axis, and β is proportional to the linear absorption coefficient. In fact, we use the original matrix formalism [19]: the system is described as a succession of slabs of constant electron density. The analysis of the reflectivity profile gives the reduced electron density δ, the thickness and the roughness of each slab.

The main advantage of free-standing films arises from the high electron density gradient at both air-film interfaces. X-ray reflectivity curves display very strong Kiessig fringes that originate from the interference of the beams reflected on each side of the film whereas reflectivity profiles on the surface of a solution do not exhibit such a contrast. The film drainage can also be followed with reflectivity profiles on a small angle area by choosing a short acquisition period (a few minutes), the film thickness being given by the position of the Kiessig fringes.

Using the experimental method described in details in previous papers [14,15], films are drawn from the amphiphilic polymer solutions by lifting a vertical metallic frame at a constant rate (2 cm/min). Reflectivity experiments are performed using a four-circle diffractometer (Micro-Controle). The x-ray wavelength is $\lambda = 1.5405$ Å ($\mathrm{Cu}\,K\alpha_1$ line) and a small vertical slit (100 μm) placed at a distance of 40 cm from the source ensures a low divergence of the beam (0.15 mrad). A horizontal slit (1.25 mm) limits the height of the illuminated area of the film.

IV. RESULTS AND DISCUSSION

First, it is highly important to determine whether the state of the solution surface (from which films are drawn) affects the drainage and the thickness of the film. This preliminary study is required to establish an experimental procedure that ensures the reproducibility of the results concerning the behavior of the films. In fact, surface-tension measurements showed that the organization of the surface of the solution is a very slow process lasting up to one day [18] (Fig. 1—inset). Such long equilibration times are explained in terms of a penetration of alkyl grafts through the adsorbed layer. To test the influence of the surface organization, films were drawn from a 3% concentrated 120 1C12 ($M_W = 120 \times 10^{+3}$, $\tau = 1$, $n = 12$) copolymer solution (a concentration lower than cac) after having left the surface of the solution at rest for various lengths of time ranging from one hour to one day. The thinning and lifetime of the films are then investigated as a function of the resting time of the surface (Fig. 1). The longer the surface equilibrates, the slower the drainage: a thickness of 475 Å (here the equilibrium is still not reached) is obtained after, respectively, one and three hours for films drawn from solutions left at rest for one hour and one day. The average lifetime and the rate of thinning of the

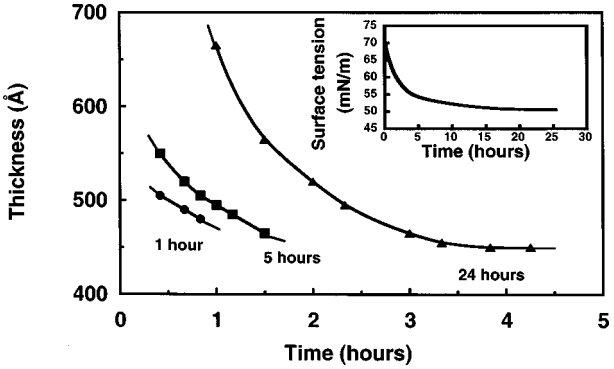

FIG. 1. Drainage of a film drawn from a 120 1C12 solution at a concentration of 3 wt.% after the solution had been left undisturbed for increasing lengths of time: ●, 1 hour; ■, 5 hours; ▲, 24 hours. Inset: surface tension of the same solution as a function of time.

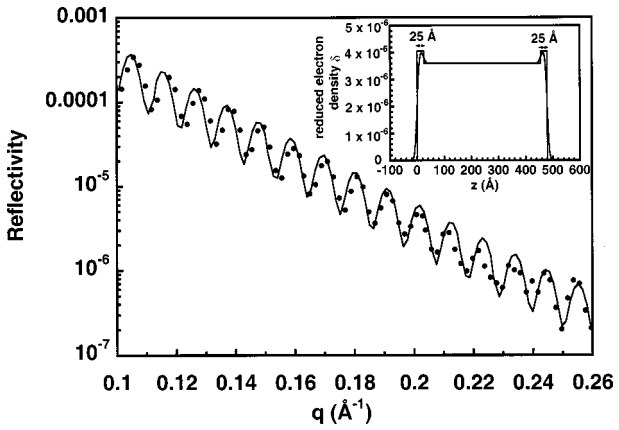

FIG. 2. Experimental reflectivity curve of a 120 1C12 copolymer film (circles) and the best fit (solid line) using a three slab-model. Inset: reduced electronic density profile obtained from the best fit. The step and the real profiles are represented. Contrary to the step profile, the real profile does not present any discontinuity of $\delta(z)$. As a matter of fact, the discontinuities are smoothed by the roughness of the interfaces between the slabs. A monomer units-rich zone of thickness 25 Å is detected at the air/film interfaces.

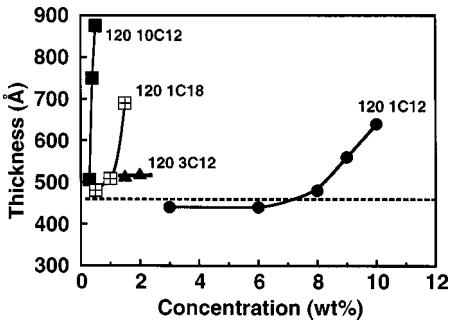

FIG. 3. Concentration dependence of the film equilibrium thickness for various degrees of grafting (τ) and lengths of the grafts (n) at a constant molecular weight ($M_W = 120\,000$ g/mol): ●, 120 1C12; ▲, 3C12; ■, 10C12; ⊞, 1C18.

films, respectively, increases and decreases with the degree of order of the solution surface. When the film lifetime is long enough, an equilibrium thickness can be defined since the drainage stops when a thickness of 440 ± 5 Å is reached. In the following, we have then waited for one day (typically the time of organization of the adsorbed layer) before drawing the films so that they could last longer and we could have reproducible experimental conditions to follow the thinning of the film and to determine its equilibrium thickness.

This experimental procedure being established, we investigated the electron-density profile within this film. Once the drainage was completed, a scan with a long acquisition period (24 hours) was performed to improve the accuracy of the reflectivity profile and to evidence an electron density gradient. Figure 2 shows an experimental curve (circles) for a film drawn from a 8% 120 1C12 solution. Strong Kiessig fringes are displayed that proves that there exists a good parallelism between the two faces of the film. The experimental curve cannot be fitted with a single-slab model, corresponding to a homogeneous film. A three-slab model is then required in which the outer slabs correspond to dense layers of adsorbed polymer molecules at the air-film interfaces. The reduced electron-density profile obtained from the best fit is represented in Fig. 2—inset. These outer layers provide the elasticity of the film as in any kind of amphiphilic molecule film and have been described theoretically [4] and evidenced experimentally [8] for adsorbed polymers. From the best theoretical fit (solid line in Fig. 2), we obtain a thickness of 25 ± 5 Å and a reduced electron density of $(4.05 \pm 0.05) \times 10^{-6}$ for these layers. The polymer volume fraction Φ can be calculated through the relation:

$$\Phi = (\delta - \delta_{\text{water}})/(\delta_{\text{polymer}} - \delta_{\text{water}}), \qquad (2)$$

where δ_{water} is the water reduced electron density (3.56×10^{-6}) and δ_{polymer} is the reduced electron density of the pure polymer (4.7×10^{-6}). We found $\Phi = 40 \pm 5\%$. The core of the film (430 ± 5 Å) corresponds to polymer molecules that extend from the interface to the aqueous sublayer. Its reduced electron density is found to be equal to that of water within fitting uncertainty, which shows that the polymer concentration in the core is lower than that in the outer layers. To limit the number of fitting parameters, we have imposed the same roughness at the air/outer slab and outer slab/film-core interfaces. This roughness (6 ± 0.5 Å) is larger than that of films made of low molecular weight surfactants (3 Å in Ref. [14]). In this latter case, the roughness was essentially due to thermal excitation. For polymer films, an additional roughness (3 Å) takes place. In addition, x-ray reflectivity measurements were carried out on the surface of the corresponding solution [18]. The same thickness was obtained (25 ± 2 Å) for the monomer units–rich zone and the sublayer was not detected because the electron density of the polymer molecules is close to that of the solvent.

Alternatively, we have deduced the behavior of the polymer in the core of the film by varying the parameters of the polymer and its concentration in the initial solution: it is the first important result of this paper. A single x-ray reflectivity curve does not permit us to determine directly the behavior and the concentration of the polymer within the core of the film but the film thickness, which is given by the position of the Kiessig fringes, is easily and precisely measured. We then have carried out an investigation of the film equilibrium thickness (Fig. 3) by varying τ (1, 3, and 10 mol%), n (12 and 18 carbon atoms), and the polymer concentration C (wt.%), at constant molecular weight ($M_W = 120\,000$ g/mol). The existence of a concentration threshold C_t has been evidenced, below which the film thickness remains constant with concentration and is independent of τ and n (470 ± 40 Å for the whole range of τ and n). Above C_t, the film thickness increases with concentration. The values of C_t (8%, 0.3%, and 1%, respectively, for 120 1C12, 10C12, and 1C18) are close to the respective cac [1,2,18]. The increase in thickness is progressively more rapid when the degree of grafting τ is increasing. A film drawn from a 120 10C12 solution at a concentration of 0.75% remains red (a color corresponding to a thickness of about 2000 Å) during several days and does not thin further. The stop of the drainage above C_t is probably due to the aggregation process within the film. In other words, the films no longer become thinner when the adsorbed layers are connected to the bulk. Above C_t, nonadsorbed polymer molecules are trapped into the film and are linked to the adsorbed molecules via the

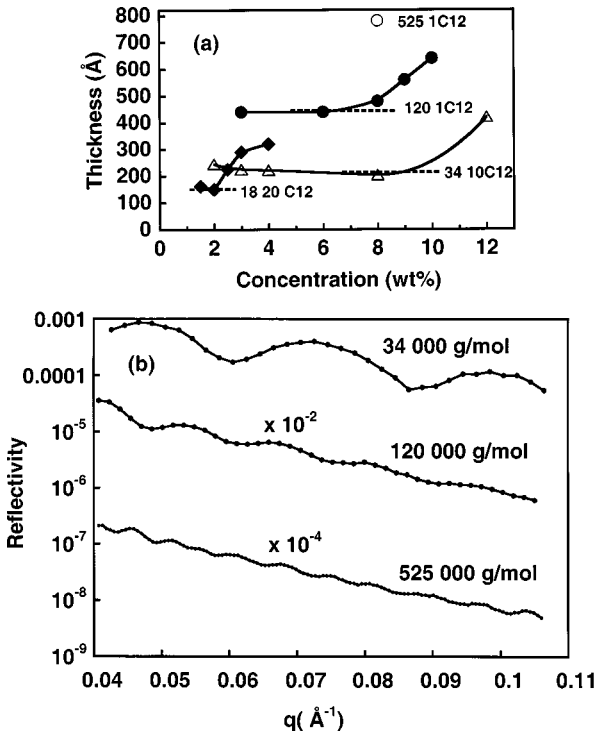

FIG. 4. (a) Concentration dependence of the film equilibrium thickness for various molecular weights of the polymer backbone: ○, 525 1C12; ●, 120 1C12; △, 34 10C12; ◆, 18 20C12. (b) Three examples of Kiessig fringes. The film thickness increases with an increase in the polymer molecular weight.

hydrophobic aggregates, thereby creating a bridge between the walls of the film. In particular, the rapid increase in thickness of 120 10C12 copolymer films above C_t could be due to the rapid increase in viscosity with concentration above cac [1,2]. Obviously, C_t is closely related to cac, though *a priori* different since the polymer concentrations within the film and in the solution are different. Nevertheless, we did not observe any difference between their values. Static light diffusion measurements [20] gave a radius of gyration in salt medium (1.75*M* NaCl) equal to about half the film thickness below C_t. We then conclude that for $C<C_t$, films are composed of solely two walls of polymer molecules in interaction, each of them being adsorbed at one side of the films. By increasing the concentration, we thus observe a transition at C_t from a bimolecular film to a nonpourable physical gel and the two faces of the film are then bridged.

The last part of this paper deals with the dependence of the film thickness on the molecular weight. As shown above, the film thickness does not depend on the degree of grafting below C_t. Hence, the 18 20C12, 34 10C12, 120 1C12, and 525 1C12 copolymers were used to study the effects of the backbone molecular weight. The thickness of films made with the 18 20C12 and 34 10C12 copolymers exhibits the concentration dependence described above with the existence of a concentration threshold [Fig. 4(a)], thus generalizing this behavior to other molecular weights. For the 525 1C12 copolymer, we have only studied a film drawn from a solution at cac (8%). Below the threshold concentration, the Kiessig fringes become larger when the polymer molecular weight is decreasing [Fig. 4(b)], indicating a decrease of the film thickness.

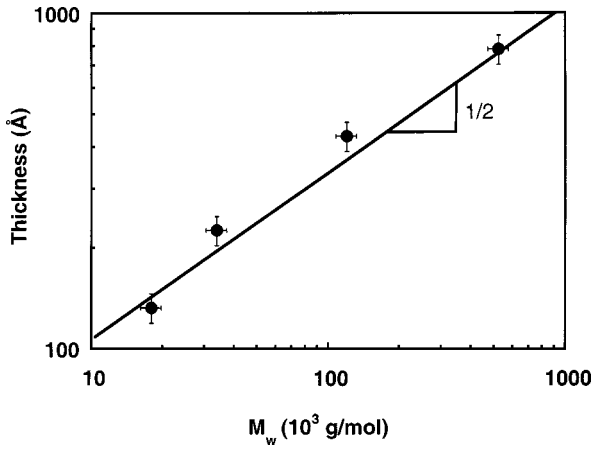

FIG. 5. Dependence of the film thickness on the polyelectrolyte weight average molecular weight M_W. The thickness scales like $M_W^{1/2}$. M_W is obtained from SEC measurements within an error of 10%. The uncertainty in the film thickness estimation for a given molecular weight is 10%.

As shown in Fig. 5, the film thickness below C_t scales like $M_W^{1/2}$. It is the well-known scaling law for the radius of gyration of Gaussian coils. As the conformation and the size of polyelectrolyte chains in aqueous solution depend largely on the polyelectrolyte concentration [21,22], it is important to estimate the average concentration of HMPAANa copolymer within the film and to determine its behavior at this concentration. For films drawn from the 120 1C12 solution concentrated at 8% (corresponding to the threshold concentration C_t), the average polymer concentration within the film is obviously higher than 8% because an adsorbed layer is more concentrated than the bulk. As the film thickness does not depend on τ, it is reasonable to assume that the organization of 120 τC12 films and their average polymer concentration are similar at their respective C_t and independent of τ. In the same way, the polymer concentration in the 34 10C12 copolymer film drawn from a 8% solution (C_t) must be at least equal to 8%. We have carried out low-shear viscosity measurements for three nongrafted precursor homopolymers (molecular weights equal to 34, 120, and 525 $\times 10^3$ g/mol) as a function of the polymer concentration (Fig. 6). At low concentration, the viscosity η follows the so-called Fuoss law ($\eta \propto C^{1/2}$) for the semidilute polyelectrolyte

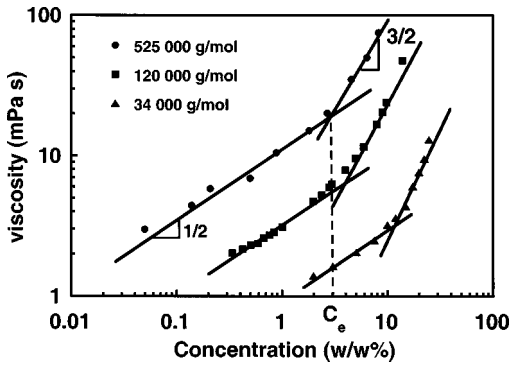

FIG. 6. Below C_e, the viscosity scales like $C^{1/2}$, characterizing the semidilute regime. Above C_e, entanglements appear between the polyelectrolyte chains and the viscosity increases more rapidly ($\eta \propto C^{3/2}$). In this regime, the chains are in a Gaussian coil conformation.

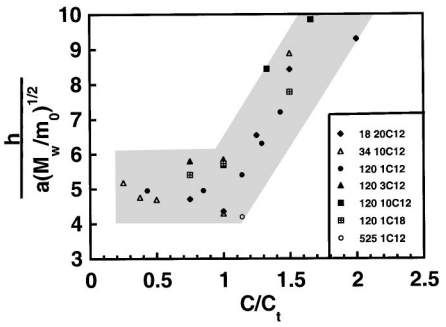

FIG. 7. Variation of the reduced film thickness with the reduced concentration C/C_t. A general feature is obtained. The film thickness h is given by the empirical expression: $h = a(M_W/m_0)^{1/2} f(C/C_t)$ where h is the film thickness, a and m_0 are the length and molecular weight of the nongrafted monomer unit, respectively, and f is an increasing function of C/C_t. The gray ribbon is a guide for the eye and represents the dispersion of the results.

solutions [23] and above a determined concentration C_e, η varies like $C^{3/2}$. The scaling law above C_e has been explained theoretically [22] and corresponds to the semidilute entangled regime, C_e being the entanglement concentration. In this regime, the polyelectrolytes chains are self-screened and adopt a Gaussian coil conformation, with a radius scaling like $M_W^{1/2}$ [22]. Comparing the C_e values (10, 5, and 3%, respectively, for the 34, 120, and 525 homopolymer precursors) with the C_t values of the grafted polymers of same molecular weight, it is concluded that polymers within the films are in the regime of entangled self-screened Gaussian coils, which explain the variations of the film thickness with the molecular weight. This finding is the second important result of this study and can be compared to the experimental results in Ref. [12] that showed that the forces between the faces of the film are controlled by the size of the polymer coils.

The coil conformation of adsorbed polyelectrolytes results from a subtle balance between the energy of adsorption, the polymer entropy, the osmotic pressure of monomers and counter-ions within the adsorbed layer, and the electrostatic repulsion between coils. An increase of salt up to $1M$ NaCl does not lead to a thinner film. This observation is consistent with theoretical results [22] predicting a low dependence of the radius of polyelectrolyte coils R_g with salt concentration C_s ($R_g \propto C_s^{-1/8}$). There is probably no electrostatic repulsion between the two walls of the film and consequently, the emulsion stabilization effect does not result from electrostatic repulsion between droplets, contrary to what is usually admitted [3]. In particular, a recent theory [24] concludes that an adsorbed polyelectrolyte layer creates a long-range electrostatic potential, contrary to our results. This theory assumes that the chains adsorb in flat conformation, which is clearly not the case in our study where the loops and tails screen the surface potential with their counterions and form coils that determine the film thickness.

Finally, it is convenient to introduce the reduced thickness $(h/a)(M_W/m_0)^{1/2}$ where h is the film thickness, a and m_0 are, respectively, the length and molecular weight of the nongrafted monomer unit. The reduced thickness is a general function of the reduced concentration C/C_t (Fig. 7). This tends to show that the film structure is similar for all samples

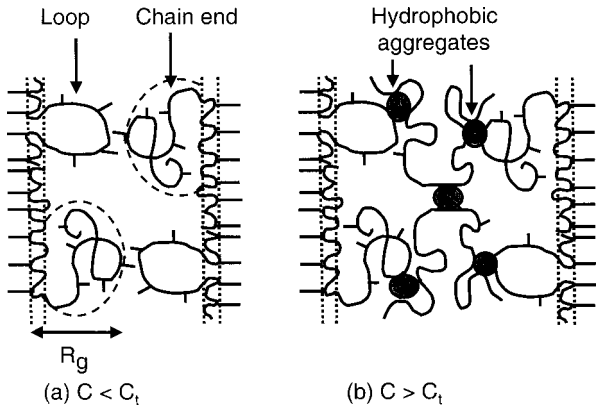

FIG. 8. Schematic representation of the structure of an amphiphilic associating polyelectrolyte film. (a) $C<C_t$: the radius of gyration determines the film thickness. (b) $C>C_t$: the adsorbed molecules are connected to the bulk via the hydrophobic aggregates. The film thickness increases rapidly with concentration. A transition from a bimolecular film to a nonpourable physical gel occurs.

regardless of their size and their structure. A schematic representation of the film can then be proposed: below C_t [Fig. 8(a)], the film thickness is governed by the radius of gyration of the coils and above C_t [Fig. 8(b)], aggregation occurs within the film and its thickness rapidly increases.

V. CONCLUSION

In summary, we have carried out an overall investigation of films of amphiphilic polyelectrolytes by varying a broad range of parameters of the polymer in the range of concentration in which the films are stable. We have evidenced thin layers of adsorbed polymer on both sides of the film. At a determined concentration threshold, a transition from a bimolecular film to a physical gel has been observed. Below the threshold, the film thickness is solely governed by the polyelectrolyte molecular weight and is proportional to the radius of gyration. Moreover, we found that an addition of salt does not change the film thickness. No electrostatic repulsion seems to occur between the walls of the film because the Debye length is small compared to the polymer size and consequently, adsorbed polyelectrolyte chains self-screen. Above the concentration threshold, the film thickness rapidly increases with concentration and a physical gel is formed. Fluorescence experiments should be useful to confirm the existence of hydrophobic aggregates within the films. In the case of macroemulsions, the oil droplets are trapped in a physical network of hydrophobic aggregates and they cannot come into contact. The formation of a physical gel between droplets is thus a key factor in explaining the efficient macroemulsion stabilization by HMPAANa [1,2]. Hence, we have related a microscopic investigation of copolymer films and macroscopic observations of macroemulsions. Polymer films are shown to be very appropriate systems for a better understanding of the stabilization process.

ACKNOWLEDGMENTS

We are very grateful to P. G. de Gennes, M. Daoud, F. Lafuma, O. Mondain-Monval, and J. A. Hodges for extremely fruitful discussions. We would like to thank Nicolas Cuvillier for his kind help in the data treatment.

[1] P. Perrin and F. Lafuma, J. Colloid Interface Sci. **197**, 317 (1998).
[2] P. Perrin, F. Lafuma, and R. Audebert, Prog. Colloid Polym. Sci. **105**, 228 (1997).
[3] D. H. Napper, *Polymeric Stabilization of Colloidal Dispersions* (Academic, New York, 1983).
[4] P. G. de Gennes, Macromolecules **14**, 1637 (1981); *Scaling Concepts in Polymer Physics* (Cornell University Press, London, 1979); Macromolecules **15**, 492 (1982).
[5] J. M. H. M. Scheutjens and G. J. Fleer, J. Phys. Chem. **84**, 178 (1980).
[6] A. N. Semenov, J. Bonet-Avalos, A. Johner, and J. F. Joanny, Macromolecules **29**, 2179 (1996); **30**, 1479 (1997).
[7] S. Alexander, J. Phys. (Paris) **38**, 983 (1977).
[8] L. T. Lee, O. Guiselin, B. Farnoux, and A. Lapp, Macromolecules **24**, 2518 (1991).
[9] B. Demé and L. T. Lee, J. Phys. Chem. B **101**, 8250 (1997).
[10] J. Israelachvili, *Intermolecular and Surface Forces* (Academic, San Diego, 1985).
[11] H. J. Taunton, C. Toprakcioglu, L. J. Fetters, and J. Klein, Nature (London) **332**, 712 (1988).
[12] O. Mondain-Monval, A. Espert, P. Omarjee-Rivière, J. Bibette, F. Leal Calderon, J. Philip, and J. F. Joanny, Phys. Rev. Lett. **80**, 1778 (1998).
[13] P. Auroy, L. Auvray, and L. Leger, Phys. Rev. Lett. **66**, 719 (1991).
[14] O. Bélorgey and J. J. Benattar, Phys. Rev. Lett. **66**, 313 (1991).
[15] P. Guenoun, A. Schlachli, D. Sentenac, J. W. Mays, and J. J. Benattar, Phys. Rev. Lett. **74**, 3628 (1995).
[16] T. K. Wang, I. Iliopoulos, and R. Audebert, Polym. Bull. (Berlin) **20**, 577 (1989).
[17] F. Petit, I. Iliopoulos, and R. Audebert, Polymer **39**, 751 (1998).
[18] F. Millet, M. Nedyalkov, B. Renard, P. Perrin, F. Lafuma, and J. J. Benattar, Langmuir **15**, 2112 (1999).
[19] M. Born and E. Wolf, *Principles of Optics*, 6th ed. (Pergamon, London, 1984), p. 51.
[20] B. Magny, thesis, University of Paris, 1992 (unpublished).
[21] P.-G. de Gennes, P. Pincus, R. M. Velasco, and F. Brochard, J. Phys. (Paris) **37**, 1461 (1976).
[22] A. V. Dobrynin, R. H. Colby, and M. Rubinstein, Macromolecules **28**, 1859 (1995).
[23] S. Förster and M. Schmidt, Adv. Polym. Sci. **120**, 51 (1995).
[24] M. A. Cohen Stuart, C. W. Hoogendam, and A. de Keizer, J. Phys.: Condens. Matter **9**, 7767 (1997).